Finite Elements in Analysis and Design 45 (2009) 555–568

Contents lists available at ScienceDirect

Finite Elements in Analysis and Design

journal homepage: www.elsevier.com/locate/finel

Using artificial reaction force to design compliant mechanism with multiple equality displacement constraints

Zhenyu Liu[a,*], Jan G. Korvink[b]

[a]State Key Laboratory of Applied Optics, Changchun Institute of Optics, Fine Mechanics and Physics (CIOMP), Chinese Academy of Sciences, Changchun, Jilin 130033, China
[b]Laboratory for Simulation, Department of Microsystems Engineering (IMTEK), and Freiburg Institute of Advanced Studies (FRIAS), University of Freiburg, 79110 Freiburg, Germany

ARTICLE INFO

Article history:
Received 6 September 2007
Received in revised form 18 March 2009
Accepted 23 March 2009
Available online 8 May 2009

Keywords:
Topology optimization
Compliant mechanism
Equality constraint
Reaction force
Mesh adaptation

ABSTRACT

Monolithic compliant mechanisms are elastic workpieces which transmit force and displacement from an input position to an output position. Continuum topology optimization is suitable to generate the optimized topology, shape and size of such compliant mechanisms. The optimization strategy for a single input single output compliant mechanism under volume constraint is known to be best implemented using an optimality criteria or similar mathematical programming method. In this standard form, the method appears unsuitable for the design of compliant mechanisms which are subject to multiple outputs and multiple constraints. Therefore an optimization model that is subject to multiple design constraints is required. With regard to the design problem of compliant mechanisms subject to multiple equality displacement constraints and an area constraint, we here present a unified sensitivity analysis procedure based on artificial reaction forces, in which the key idea is built upon the Lagrange multiplier method. Because the resultant sensitivity expression obtained by this procedure already compromises the effects of all the equality displacement constraints, a simple optimization method, such as the optimality criteria method, can then be used to implement an area constraint. Mesh adaptation and anisotropic filtering method are used to obtain clearly defined monolithic compliant mechanisms without obvious hinges. Numerical examples in 2D and 3D based on linear small deformation analysis are presented to illustrate the success of the method.

1. Introduction

The design of monolithic compliant mechanisms using structural topology optimization is an innovative method capable of designing novel actuators and sensors [1]. The important advantages of compliant mechanisms, when compared with rigid mechanisms with joints, are that a single piece does not require assembly, that friction is reduced, and that a built-in restoring force automatically. These characteristics make compliant mechanisms widely applicable in those areas where device assembly is not practicable, i.e. in microtechnology [2]. The simplest design of compliant mechanisms can be summarized as the *single-input–single-output* (SISO) type subject to a material volume constraint, and a straightforward implementation has been demonstrated in [3] using the *optimality criterion* (OC) method. However, designing for more practical actuator requirements can seldom be expressed as an SISO model, and instead we have *multiple-input–multiple-output* (MIMO) devices subject to multiple constraints, such as displacement and stress, together with material volume constraint. In this case, an advanced optimization method with a suitable objective function is necessary to obtain an optimized structure which can fulfill all the design necessities. Much of the pioneering work on topology optimization of compliant mechanisms was proposed by Ananthasuresh [4], Frecker [5], Sigmund [6,7], Saxena [8], and Pedersen [10], among others.

In this paper, we firstly review several existing objective functions and the optimization methods which are commonly used for the design of compliant mechanisms with specified constraints. As an alternative to these existing methods, the *artificial reaction force* (ARF) method is then proposed to implement compliant mechanism design with *equality displacement constraint* (EDC). Possible extensions of the proposed method are also discussed.

2. Survey of existing methods for the design of compliant mechanisms

There are two different design objectives which need to be satisfied simultaneously when designing a compliant mechanism. First,

* Corresponding author.
E-mail address: zhenyu_ciomp@hotmail.com (Z. Liu).

0168-874X/$ - see front matter © 2009 Elsevier B.V. All rights reserved.
doi:10.1016/j.finel.2009.03.005

Nomenclature

$c(x)$	general objective function
f_{in}	scalar force at the input point
f_{out}	scalar force at the output point
f_{RIiX}	reaction forces corresponding to the slack displacement u^*_{IiX}
f_{ROiX}	reaction forces corresponding to the slack displacement u^*_{OiX}
$h(x)$	general equality constraint
$g(x)$	general inequality constraint
k_e	element stiffness matrix
k_{in}	scalar coefficient of spring stiffness on the input point
k_{out}	scalar coefficient of spring stiffness on the output point
l_{IiX}	column vector with value of 1 corresponding to u_{IiX} and zero at other components
l_{OiX}	column vector with value of 1 corresponding to u_{OiX} and zero at other components
u_{in}	scalar displacement along the direction of f_{in} on the input point
u_{out}	scalar displacement on the main output point
u_{IiX}	displacements along $X \in (x,y,z)$ direction for i-th input point; u_{IiX} includes three components, u_{Iix}, u_{Iiy}, u_{Iiz}, for three-dimensional case
u_{OiX}	displacements along X direction for i-th output point
u^*_{IiX}	slack displacements along X direction for i-th input point
u^*_{OiX}	slack displacements along X direction for i-th output point
ARF	artificial reaction force
B	element strain matrix
CONLIN	convex linearization method
D	material elastic matrix
EDC	equality displacement constraint
F	load vector
K	discretized global stiffness matrix which is used to calculate true displacement vector *U* of compliant mechanism
K_{RF}	discretized global stiffness matrix which is used to calculate artificial displacement vector U_{RF} and artificial reaction forces F_{RIiX} and F_{ROiX}
K_{SE}	discretized global stiffness matrix which is used to calculate displacement U_{SE}
L	augmented objective function
MIMO	multiple input multiple output
MMA	method of moving asymptotes
MSE	mutual strain energy
P	penalty parameter for the SIMP method
SE	strain energy
SISO	single input single output
SLP	sequential linear programming
SQP	sequential quadratic programming
U	displacement vector
U_{RF}	displacement vector which is used to calculate the artificial reaction force
U_{SE}	displacement vector which is used to calculate the value of SE
α	adjoint vector for mechanical equilibrium equation
β	diffusion time
γ	Lagrange multiplier for the area constraint
η	numerical damping coefficient for the OC method
λ	Lagrange multiplier for equality constraint
μ	penalty coefficient for equation constraint
ω	scalar weight coefficient for multiple objectives
Ω	design domain
ρ	design variable for topology optimization
$\rho_{\min}$	minimum value of design variable ρ
$\rho_{\max}$	maximum value of design variable ρ

the mechanism should be flexible enough to satisfy the kinematic requirements. Second, the mechanism should stiff enough to support an external load and to transport output force and displacement [2,8]. These two design objectives are complementary to each other. An optimum balance between flexibility and stiffness is a key point to be resolved in designing compliant mechanisms. Four different approaches have been proposed to balance the flexibility and stiffness necessities. Sigmund proposed using single output displacement as objective function [3] (Fig. 2):

$$\begin{aligned} \max \quad & u_{out} \\ \text{s.t.} \quad & KU = F \end{aligned} \tag{M1}$$

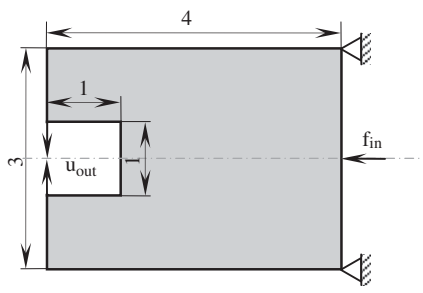

Fig. 1. Design domain and boundary condition for SISO compliant gripper.

where u_{out} is the displacement on the output point which prefers to have maximized displacement, K is the discretized global stiffness matrix using the finite element method, U is the unknown displacement vector and F is the load vector. The stiffness requirements of the whole structure can be adjusted through the stiffness of springs k_{in} and k_{out} placed on the input and output parts [17]. Anathasuresh proposed the weighted sum of *mutual strain energy* (MSE) which is numerically equal to the output displacement u_{out}, and *strain energy* (SE) which is used to measure the stiffness of the compliant mechanism [4] (Fig. 3):

$$\begin{aligned} \max \quad & \omega \ \text{MSE} + (1-\omega)\ \text{SE} \\ \text{s.t.} \quad & KU = F \end{aligned} \tag{M2}$$

where ω is the weight coefficient. Because this is a bi-objective formulation, the optimized compliant mechanism may be different when choosing different weighted coefficients. Therefore Frecker suggested to use the ratio of MSE and SE as the objective [5] (Fig. 3):

$$\begin{aligned} \max \quad & \frac{\text{MSE}}{\text{SE}} \\ \text{s.t.} \quad & KU = F \end{aligned} \tag{M3}$$

When using the ratio of two design objectives rather than a linear combination as the objective, it can avoid the difficulty of the Pareto problem for a multi-objective optimization problem [9]. To consider the output work, Sigmund proposed to use the mechanical advantage

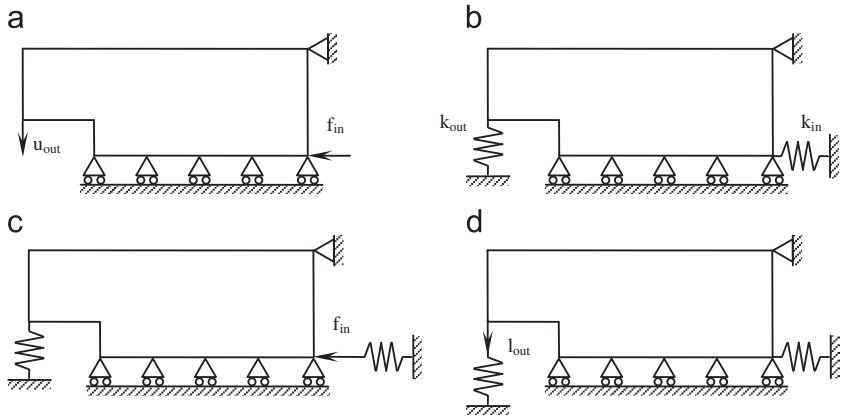

Fig. 2. The model M1 for design of compliant gripper based on Fig. 1. (a) Design domain, input force and objective of output displacement, (b) spring model, (c) model to solve the displacement vector, (d) model to solve the adjoint vector.

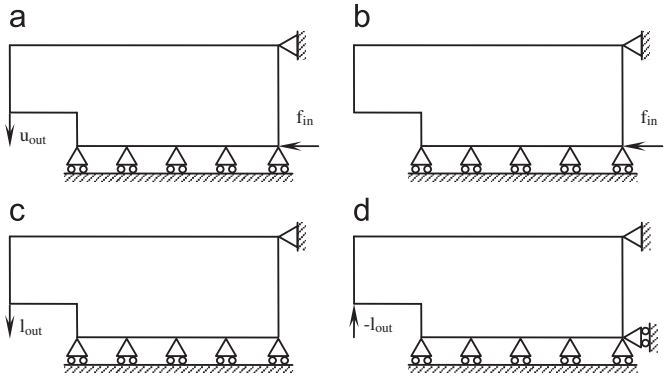

Fig. 3. The model M2 and M3 for design of compliant gripper based on Fig. 1. (a) Design domain, input force and objective of output displacement, (b) model to solve the displacement vector, (c) model to solve the adjoint vector, (d) model to solve the strain energy.

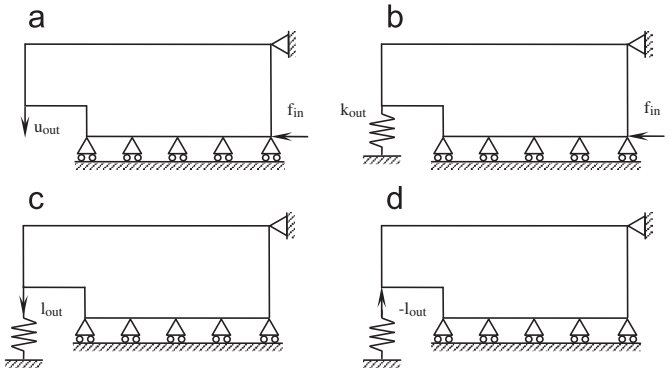

Fig. 4. The model M4 for design of compliant gripper based on Fig. 1. (a) Design domain, input force and objective of output displacement, (b) model to solve the displacement vector, (c) model to solve the adjoint vector, (d) model to solve the strain energy.

(the ratio of output force and input force) with constraint by the input displacement [6]

$$\begin{aligned} \max \quad & \frac{f_{out}}{f_{in}} \\ \text{s.t.} \quad & KU = F \end{aligned} \tag{M4a}$$

where $f_{out} = k_{out} \cdot u_{out}$ is the output (reaction) force on the output point, and f_{in} is the input force added at the input point. Saxena also proposed to use an energy based objective (the ratio of square of MPE and SE) [8] (Fig. 4):

$$\begin{aligned} \max \quad & \frac{0.5 k_{out}\ \mathrm{MSE}^2}{\mathrm{SE}} \\ \text{s.t.} \quad & KU = F \end{aligned} \tag{M4b}$$

Note that, for the optimization models M1–M4, the extra constraints are not shown in the text so as to simplify the expressions.

Parallel to these objective models, there are several mathematical programming methods which are suitable for structural topology optimization with given constraints. The *optimality criteria* method finds the optimal solution by solving the equation of optimal condition. For the case when just one single geometrical constraint, such as the material volume, needs to be constrained, this method is straightforward to use for the design of compliant mechanisms [3]. The second type of methods are *sequential linear programming* (SLP) and *sequential quadratic programming* (SQP) methods. These are classical methods from the mathematical programming viewpoint, and are able to solve smooth, nonlinear constrained optimization problems. The original nonlinear objective function is approximated using a sequence of simpler linear or quadratic forms [18]. For structural topology optimization with several constraints, together with lower and upper bound limitations for each design variable, the *convex linearization* (CONLIN) method [12] and its extension *method of moving asymptotes* (MMA) [11] are commonly used in recent years. Similar to the SLP and SQP methods, the CONLIN method also approximates the original objective function using a sequence of subproblems. However, these subproblems are separable and convex, and are constructed using the sensitivity and the value of objective function at the current iteration point as well as for several subsequent iterations [14]. Except for these mathematical programming methods, other global type optimization methods, such as the genetic algorithm, are also discussed [15,16].

For designing compliant mechanisms with multiple constraints, the MMA type methods are widely used. Originally, the MMA is used to optimize an objective function $c(x)$ together with inequality constraints $g_j(x)$:

$$\begin{aligned} \min \quad & c(x) \\ \text{s.t.} \quad & g_j(x) \leqslant 0, \quad j = 1, \ldots, n \end{aligned} \tag{1}$$

Here n represents the number of constraints. Equality constraints normally can be categorized into two groups. The first are only associated with the geometrical properties of the optimization problem, such as a volume constraint, and smoothness of the structural

boundaries. The second are often associated with forward physical problems, such as displacement and stress constraints for the mechanical problem. For the first group of equality constraints, the approximation of the constraints does not require a numerical analysis of the forward problem. Therefore they can be fulfilled separately from second group of equality constraints, or even other inequality constraints, and using an optimization method with lower computational cost [13]. For the second group of equality constraints, the approximation of constraints requires costly finite element analysis, or some other numerical methods to evaluate the violation of equality constraints, which mean that they cannot be implemented as simple as the first group. To extend the MMA method to problems with equality constraints $h_i(x)$:

$$\begin{aligned} &\min \quad c(x) \\ &\text{s.t.} \quad h_i(x)=0, \quad i=1,\dots,m \end{aligned} \tag{2}$$

Sigmund suggested to approximate the equality constraints using inequality constraints:

$$\begin{aligned} &\min \quad c(x) \\ &\text{s.t.} \quad h_i^2(x)\leqslant \varepsilon, \quad i=1,\dots,m \end{aligned} \tag{3}$$

where ε is a small positive number [7]. The ε can be chosen as a reasonable larger number at the beginning of the optimization procedure, which is then decreased continuously to a reasonably smaller number. This strategy can also be used for both groups of equality constraints in most cases. However, the magnitude of the different equality constraints may vary by several orders of magnitude, one may need to calibrate the sensitivity for different equality constraints.

3. Design of compliant mechanism with equality displacement constraints

In this paper, we restrict our focus on the optimization of compliant mechanisms with EDCs for the purely mechanical problem with a fixed load vector. The deformation of the compliant mechanism is assumed to be very small so that one can use linear deformation analysis. The optimization model u_{out}/SE, which is similar to MSE/SE (M3), and the OC method are used to implement compliant mechanism design with EDCs. We will first derive the sensitivity of the optimization problem using the standard Lagrange multiplier method. Then we propose a novel numerical method to implement the sensitivity analysis with multiple EDCs based on the Lagrange multiplier method.

3.1. Augmented Lagrangian method

One commonly used optimization method which can deal with equality constraints is the Lagrangian method, in which the equality constraints are added into the original objective function using Lagrange multipliers λ_i:

$$L_1(u,\lambda_i)=f(u)-\sum_{i=1}^{m}\lambda_i h_i(u) \tag{4}$$

Here the Lagrange multipliers are treated as independent variables, and are calculated at each step of the optimization procedure. The quality of equality constraints strongly depends on the accuracy of the Lagrange multipliers. Another important method for constrained optimization is the quadratic penalty method. It replaces the constraints by penalty terms into the objective function, where each penalty term is a multiple of the square of the constraints violation:

$$L_2(u,\mu_i)=f(u)+\frac{1}{2}\sum_{i=1}^{m}\frac{h_i^2(u)}{\mu_i} \tag{5}$$

where μ is the penalty parameter. By driving μ close to zero, one penalizes the constraint violations with increasing severity. It is known that the quadratic penalty function is not exact. It has some disadvantages when μ becomes small, even though the method is often used in textbooks because of its simplicity and intuitive appeal [18].

One improved optimization method is to add both the quadratic penalty terms and Lagrange multiplier terms into the objective function, which is then referred to as the augmented Lagrangian method:

$$L(u,\lambda_i,\mu_i)=f(u)-\sum_{i=1}^{m}\lambda_i h_i(u)+\frac{1}{2}\sum_{i=1}^{m}\frac{h_i^2(u)}{\mu_i} \tag{6}$$

This method can reduce the possibility of ill conditioning of the quadratic penalty term by adding explicit Lagrange multiplier estimates into the objective function to be minimized. Another important property of this method is that one can obtain the minimizer of the original constraint optimization problem by minimizing the augmented objective function L even when μ_i is not particularly close to zero, provided that λ_i is a reasonable estimate of the exact Lagrange multipliers.

In order to implement compliant mechanism structural topology optimization, one can derive the design sensitivity using the standard adjoint method. The objective function, where the output displacement of the main output point, can be expressed as $u_{out}=l_{out}^T U$, where l_{out} is a vector with the value 1 at the degree of freedom (*dof*) corresponding to the main output point and with zero at all other components, and U is the displacement vector. A formal statement of the optimization problem with one equality displacement constraint along the y-direction between the main output point and the other output point (Fig. 5) is

$$\begin{aligned} &\max \quad u_{out} \\ &\text{s.t.} \quad KU=F \\ &\qquad u_{out}-u_{O2y}=0 \\ &\qquad \int_\Omega \rho_i\, d\Omega = Vol^\Omega, \quad 0<\rho_{\min}\leqslant\rho\leqslant 1.0 \end{aligned} \tag{P1}$$

For P1, the expression for the augmented Lagrangian is

$$\begin{aligned} L(u,\alpha,\lambda,\mu)=l_{out}^T U+\alpha^T(KU-F)-\lambda(l_{out}^T U-l_{O2y}^T U) \\ +\frac{1}{2\mu}(l_{out}^T U-l_{O2y}^T U)^2 \end{aligned} \tag{7}$$

where α and λ are Lagrange multipliers for the linear equilibrium equation and EDC; l_{out} and l_{O2y} are vectors with a value of 1 at the *dofs* corresponding to the y-displacement at the main output point and the other point with equality constraint. Here the volume constraint is not included into the Lagrangian expression. It will be considered using the optimality criteria algorithm separately.

When F is a design independent load, the sensitivity of Eq. (7) is

$$\begin{aligned} \frac{\partial L}{\partial \rho_i}=l_{out}^T\frac{\partial U}{\partial \rho_i}+\alpha^T\frac{\partial K}{\partial \rho_i}U+\alpha^T K\frac{\partial U}{\partial \rho_i}-\lambda(l_{out}^T-l_{O2y}^T)\frac{\partial U}{\partial \rho_i} \\ +\frac{u_{o1y}-u_{o2y}}{\mu}(l_{out}^T-l_{O2y})\frac{\partial U}{\partial \rho_i} \end{aligned} \tag{8}$$

where $u_{out}=l_{out}^T U$ and $u_{O2y}=l_{O2y}^T U$ are the displacements at the two output points. Because the equilibrium equation is solved before the sensitivity analysis, α is an arbitrary, fixed vector. So we can rearrange the sensitivity (Eq. (8)) as

$$\frac{\partial L}{\partial \rho_i}=\alpha^T\frac{\partial K}{\partial \rho_i}U \tag{9}$$

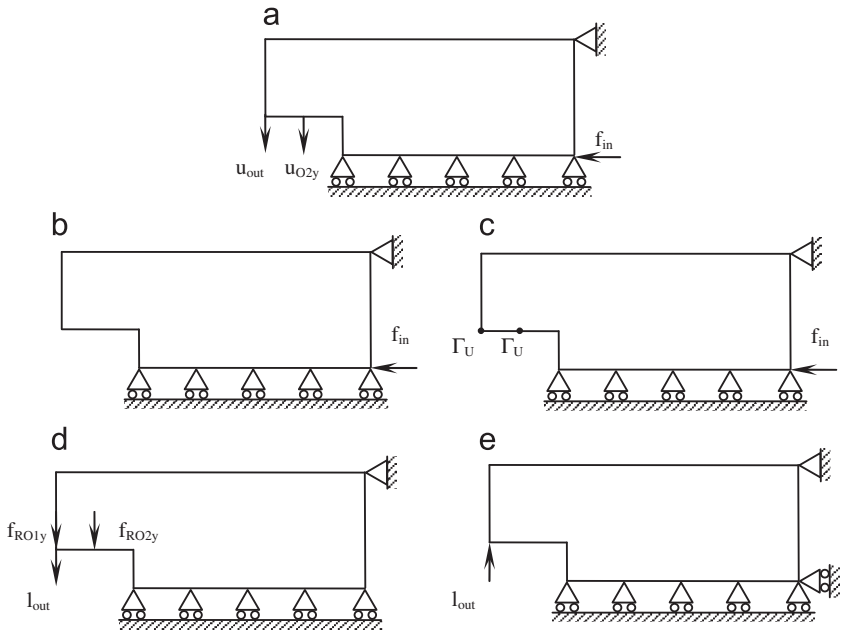

Fig. 5. The model proposed in this paper for design of compliant gripper based on Fig. 1.

where the terms which include $\partial U/\partial \rho_i$ are removed by solving the adjoint equation

$$K\alpha = -l_{out} + \left(\lambda - \frac{u_{out} - u_{O2y}}{\mu}\right) l_{out} - \left(\lambda - \frac{u_{out} - u_{O2y}}{\mu}\right) l_{O2y} \tag{10}$$

This completes the derivation of the design sensitivity for P1 using the augmented Lagrangian method. Even though the sensitivity (Eq. (9)) has the same expression compared with the case without equality displacement constraint, the adjoint vector α is solved by using additional two forces, $(\lambda - (u_{out} - u_{O2y})/\mu)l_{out}$ and $(\lambda - (u_{out} - u_{O2y})/\mu)l_{O2y}$, which are both related with the Lagrange multiplier λ and the difference of displacement on the two points with EDC. Therefore, the main challenge for the design of compliant mechanism with EDC is to calculate the additional forces which act on the constrained points.

3.2. Artificial reaction force method

The key idea of this paper is built upon the Lagrange multiplier method with modified expression of the EDCs. We will derive the design sensitivity using the standard adjoint method, and then use ARF to calculate the adjoint vector. For a compliant mechanism design with multiple constraints of displacement, the Lagrangian for the objective and constraints can be expressed as

$$L(u,\alpha,\lambda) = l_{out}^T U + \alpha^T (KU - F) - \sum_{i=1}^{m} \lambda_i (l_{OiX}^T U - u_{OiX}^*) - \sum_{j=1}^{n} \lambda_j (l_{IjX}^T U - u_{IjX}^*) \tag{11}$$

where u_{OiX}^* and u_{IjX}^* are the slack displacements which is introduced additionally to implement the displacement constraint at the different output and input points. Therefore, the adjoint equation of Eq. (11) is

$$K\alpha = -l_{out} - \sum_{i=1}^{m} \lambda_i l_{OiX}^T - \sum_{j=1}^{n} \lambda_j l_{IjX}^T \tag{12}$$

In most cases, it is not straightforward to obtain accurate Lagrange multipliers in which ensure that the optimization procedure converges smoothly. Now, we note that the load vector of Eq. (10) includes the adjoint force at two points with displacement constraints. Based on our knowledge of finite element theory, we know that the Lagrange multiplier for a point with a displacement constraint is simply the reaction force at this point [28,29]. Or stated differently, if one limits the displacement of two separate different points through a fixed relationship, then one can obtain corresponding forces which need to be added to the problem in order to satisfy the displacement constraints. Based on the above derivation, we propose a procedure in order to implement sensitivity analysis for the compliant mechanism design with EDCs:

$$KU = F \tag{13a}$$

$$K_{RF} U_{RF} = F \tag{13b}$$

$$K\alpha_{RF} = -l_{out} + \sum_{i=1}^{m} f_{ROiX} l_{OiX} + \sum_{j=1}^{n} f_{RIjX} l_{IjX} \tag{13c}$$

The three equations in Eq. (13) are discretized linear equilibrium equations based on the finite element method. They are used to solve the displacement vector, reaction forces, and adjoint vector (Fig. 5b–e), according to the specified displacement boundary conditions and input force, respectively. Here f_{ROiX} and f_{RIjX} denote the scalar artificial reaction forces in order to satisfy the equality displacement constraints. Eq. (13a) is used to solve the original displacement U (Fig. 5b). The displacement boundary conditions, which are added on the constrained output and input points to Eq. (13b) (Fig. 5c), are based on the numerical solution of Eq. (13a). In all numerical examples we present in this paper, we chose $\Gamma_U = \max(|u_{OiX}|)$ (Fig. 5c), where u_{OiX} is the output displacements of Eq. (13a). When compared to using the smaller absolute values, we penalize the structure to generate a larger deformation (thereby maximizing the objective function) when calculating the reaction force at the points subject to displacement constraints. This has the similar effect as the quadratic penalty term in Eq. (7) where the corresponding term in adjoint equation (Eq. (8)) is related to the difference of the displacements between the constraint points. The reaction forces f_{OiX} and f_{IjX} at the displacement constrained points are obtained after solving

Eq. (13b), or can be obtained simultaneously with the displacement vector when using the Lagrange multiplier method to deal with the boundary condition with displacement constraints. The modified adjoint vector α_{RF} is solved using Eq. (13c) (Fig. 5d). Therefore, the sensitivity, which includes the displacement constraints, is

$$\frac{\partial L}{\partial \rho_i} = \alpha_{RF}^T \frac{\partial K}{\partial \rho_i} U \tag{14}$$

Eq. (14) has a similar form to the sensitivity of an optimization problem without displacement constraints. The physical meaning behind this method is that one can calculate the forward equation with corresponding load vector and displacement boundary conditions so that all of the equality displacement constraints are satisfied simultaneously for the displacement solution. When the reaction force, at points which have displacement constraints, does not equal to zero, it means that the equality constraints of the optimization problem are not satisfied exactly, and hence we can use these reaction forces to calculate the adjoint load vector α_{RF}. The sensitivity is calculated based on the displacement vector of the original forward problem (U in Eq. (13a)) and the modified adjoint vector (α_{RF} in Eq. (13c)). Ideally, a solution which satisfies all constraints is obtained when all of the reaction forces equal to zero, which means that all equality constraints are satisfied simultaneously.

To balance the stiffness and compliant requirement of the compliant mechanism, we modify the optimization problem (P1) as

$$\begin{aligned} \max \quad & u_{out}/\mathrm{SE} \\ \text{s.t.} \quad & KU = F \\ & K_{SE}U_{SE} = l_{out} \\ & u_{out} - u_{O2y} = 0 \\ & \int_\Omega \rho_i \, d\Omega = Vol^\Omega, \quad 0 < \rho_{\min} \leqslant \rho \leqslant 1.0 \end{aligned} \tag{P1a}$$

where $\mathrm{SE} = U_{SE}^T K_{SE} U_{SE}$ is the structural strain energy based on the displacement solution of the equilibrium equation $K_{SE}U_{Se} = l_{out}$. The sensitivity of the strain energy SE is [1]

$$\frac{\partial(\mathrm{SE})}{\partial \rho_i} = -U_{SE}^T \frac{\partial K_{SE}}{\partial \rho_i} U_{SE} \tag{15}$$

The sensitivity of the objective function in Eq. (P1a) is

$$\frac{\partial(u_{out}/\mathrm{SE})}{\partial \rho_i} = \frac{\partial L}{\partial \rho_i}\frac{1}{\mathrm{SE}} - \frac{u_{out}}{\mathrm{SE}^2}\frac{\partial(\mathrm{SE})}{\partial \rho_i} \tag{16}$$

We can extend this method to optimization problems which have different kinds of EDCs. For example, when the design goal is to design compliant gripper in which the output displacement of two output points have same value along the y-direction and zero along the x-direction, the objective model is

$$\begin{aligned} \max \quad & u_{out}/\mathrm{SE} \\ \text{s.t.} \quad & KU = F \\ & K_{SE}U_{SE} = l_{out} \\ & u_{out} - u_{O2y} = 0 \\ & u_{O1x} = u_{O2x} = 0 \\ & \int_\Omega \rho_i \, d\Omega = Vol^\Omega, \quad 0 < \rho_{\min} \leqslant \rho \leqslant 1.0 \end{aligned} \tag{P2}$$

In problem (P1)–(P4), the main output point is also the first output point with the displacement constraint, therefore $u_{out} = u_{O1y}$ in (P1). Here u_{O1x} and u_{O2x} are the displacements along the x-direction at the output points. Problem (P2) provides more limitations to the output performance as compared with problem (P1a). Eq. (13c) can be written as

$$K\alpha_{RF} = -l_{out} + (f_{RO1y}l_{O1y} + f_{RO2y}l_{O2y}) + (f_{O1x}l_{O1x} + f_{RO2x}l_{O2x}) \tag{17}$$

The zero displacement boundary conditions on the x-direction at two output points are added in Eq. (13b). We can also constrain the displacement at points where the input force acts as long as we do not eliminate all dofs (Fig. 16):

$$\begin{aligned} \max \quad & u_{out}/\mathrm{SE} \\ \text{s.t.} \quad & KU = F \\ & K_{SE}U_{SE} = l_{out} \\ & u_{out} - u_{O2y} = 0 \\ & u_{O1x} = u_{O2x} = 0 \\ & u_{I1y} = 0 \\ & \int_\Omega \rho_i \, d\Omega = Vol^\Omega, \quad 0 < \rho_{\min} \leqslant \rho \leqslant 1.0 \end{aligned} \tag{P3}$$

Here u_{I1y} is the displacement on the y-direction at the input force point. Eq. (13c) can be written as

$$\begin{aligned} K\alpha_{RF} = & -l_{out} + (f_{RO1y}l_{O1y} + f_{RO2y}l_{O2y}) + (f_{O1x}l_{O1x} + f_{RO2x}l_{O2x}) \\ & + f_{RI1y}l_{I1y} \end{aligned} \tag{18}$$

The zero displacement boundary condition on the y-direction at input point is added in Eq. (13b). For 3D problem, the number of displacement constraints will be more than the 2D case, especially if one wishes to control the output performance specifically. For the design domain which is shown in Fig. 18, the objective is the output displacement along the z-direction for the main output point, and the jaw of gripper has mere deformation along the z-direction. The optimization model is

$$\begin{aligned} \max \quad & u_{out}/\mathrm{SE} \\ \text{s.t.} \quad & KU = F \\ & K_{SE}U_{SE} = l_{out} \\ & u_{O1z} = u_{O2z} = u_{O3z} = u_{O4z} \\ & u_{Oix} = 0, \quad i = 1, \ldots, 4 \\ & u_{Ojy} = 0, \quad j = 1, \ldots, 2 \\ & \int_\Omega \rho_i \, d\Omega = Vol^\Omega, \quad 0 < \rho_{\min} \leqslant \rho \leqslant 1.0 \end{aligned} \tag{P4}$$

Here we constrain deformation at four target points (star points in Fig. 18) so that they move only along the z-direction. At the same time, the displacement along the z-direction for all four output points are the same. The u_{Oix} and u_{Oiy} are the displacement on the x- and y-directions at the output points. Eq. (13c) is modified as

$$K\alpha_{RF} = -l_{out} + \sum_{i=1}^{4} f_{Oiz}l_{Oiz} + \sum_{i=1}^{2} f_{Oiy}l_{Oiy} + \sum_{i=1}^{4} f_{Oix}l_{Oix} \tag{19}$$

The zero displacement boundary condition on the x- and y-directions at output points are added in Eq. (13b). For all of these problems (P2)–(P4), we will solve Eq. (13) but with different displacement boundary conditions for Eq. (13b) according to different equality displacement constraints. Then different reaction forces are added to calculate the modified adjoint vector α_{RF} in Eq. (13c).

4. Numerical implementation

In order to implement EDCs using the ARF method we proposed, we discuss some implementation decisions we made.

4.1. Design variable and sensitivity analysis

For typical structural topology optimizations with the SIMP method, material densities are assumed constant in each finite element, or the design variable is the element relative density. The final structural topology is depicted by discontinuous step functions

with values close to 1 (solid) or 0 (hole). Details of a typical structural topology optimization with element density design variable is described in [24]. In the topology optimization method, there is no inherent restriction on how to choose design variables. The element density is chosen merely to coincide with typical finite element calculation.

In this paper, we choose the nodal density as design variable. The element density is interpolated from the element nodal densities. It is obvious that we can use different order polynomials to interpolate the material density in an element. The interpolation functions can coincide with the element shape functions which are used to discretize the equilibrium equation, for example, such as linear interpolation for the 4-node Lagrange element and quadratic interpolation for the 8-node serendipity element [23]. When using nodal density as the design variable, the element stiffness matrix K_e is

$$K_e = \int_{\Omega_e} [(\rho_j N_j)^P \ B^T \ D \ B] \, d\Omega_e \tag{20}$$

Here N is the element shape function, B is the strain matrix, D is the elastic matrix, and P is the penalty parameter of the SIMP method used to penalize design variables with intermediate values between 0 and 1. In this paper, p=4 is used at the beginning of the optimization procedure. To obtain a clear "material–hole" structure, the value of P increases to 6 upon convergence.

The derivation of sensitivity in Section 3 is based on a discretized form of the equilibrium equations of the underlying mechanical problem. Because we choose nodal density as the design variable, the sensitivity for each design variable should use information of the element stiffness matrices and displacement values for all elements incident to a particular nodal design variable. This is different from the procedure which applies when using element density design variable, in which only one element stiffness matrix, and the displacement values at the nodal points which belong to one particular finite element, is needed to evaluate the sensitivity for one specified design variable.

4.2. Optimization method and numerical problems

In Section 3, we derived a unified sensitivity which considers all the equality displacement constraints. Therefore, only the material volume constraint needs to be considered separately. Structural topology optimization with only one constraint can be solved by several mathematical programming methods. In this paper, we use the *OC* method which was first proposed by Bendsoe [25]

$$\rho_i^{new} = \begin{cases} \max(\rho_{\min}, \rho_i - move) & \text{if } \rho_i S_i^{\eta} \leqslant \max(\rho_{\min}, \rho_i - move) \\ \rho_i S_i^{\eta} & \text{if } \max(\rho_{\min}, \rho_i - move) < \rho_i S_i^{\eta} \\ & \quad < \min(\rho_{\max}, \rho_i + move) \\ \min(\rho_{\max}, \rho_i + move) & \text{if } \rho_i S_i^{\eta} \geqslant \min(\rho_{\max}, \rho_i + move) \end{cases} \tag{21}$$

Here *move* is positive move limit, η is numerical damping coefficient, and S_i is sensitivity including the area constraint

$$S_i = \frac{-\partial c/\partial \rho_i}{\gamma \partial V/\partial \rho_i} \tag{22}$$

where γ is a Lagrange multiplier for the area constraint. This method is widely used in many research papers when considering structural topology optimization problems subject to a single constraint. When using Eq. (21) to implement the compliant mechanism design, the sensitivity of the objective function may have both positive and negative values. Sigmund [3] proposed to modify the update rule as

$$S_i = \frac{\max(0, -\partial c/\partial \rho_i)}{\gamma \partial V/\partial \rho_i} \tag{23}$$

so that a fairly stable convergence can be obtained.

There are two parameters which may influence the convergence of the OC method, one is the damping coefficient η and the other is the allowed maximum change of the design variable in each iteration *move*. In [3], authors suggested to use η=0.3 and small value of *move* for the SISO compliant mechanism design. Based on authors' limited numerical experience, the damping coefficient is chosen as 0.2 for 2D examples and 0.1 for the 3D example. These two values works quite robust for the examples listed in this paper. In the case that there has numerical oscillation at the beginning of the optimization procedure, one can choose even smaller value of *move*. In short sum, the smaller value of the η and *move* makes the optimization procedure more stable than the large value case. However, the price we pay is the more iteration loops needed to obtain a converged solution.

Checkerboard patterns and mesh-dependencies are two well-known numerical problems which arise during topology optimization. There are a range of papers discussing the essence of these numerical problems, and several efficient methods have been proposed to overcome them [19,20]. In this paper, a simple strategy called the filter method is used to avoid these two numerical problems. To obtain a structural topology with smooth boundary without numerical oscillation, sensitivity and density values are filtered before and after updating the nodal design variable. For the design of compliant mechanisms, hinge-like features may occur when using element density design variables. This is also the situation for the nodal density design method, where design variables with intermediate values are located in structural parts which heavily influence the deformation of mechanisms. There are also several papers that focus on the solution to this problem [17]. In this paper, we try to avoid hinge-like structures using a density filter together with mesh adaptation. At the same time, we use a low ratio of material volume constraints so that the optimization results in monolithic mechanisms without seriously "weak" parts. The method which avoids hinge-like structures is based on numerical experience and is stated without theoretical proof.

4.3. Mesh adaptation

Generally, the design domain is discretized once only using regular mesh during topology optimization. The entire iteration procedure is then performed using this fixed mesh. The position and smoothness of boundary strongly depends on the mesh density. Thus one has to use a reasonable number of finite elements inside the design domain in order to balance computational cost and accuracy of the resulting structural layout. Mesh adaption has become an indispensable tool for the accurate and cost-effective numerical solution of partial differential equations. A dense mesh density is often required over the physical domain to resolve physical phenomena accurately. Adaptive meshing, which maintains a high mesh density locally in regions of material boundaries, or large solution variations, is attractive and will obviously improve the computational accuracy [21,32]. In this paper, the design domain is discretized using linear triangular elements in 2D and tetrahedral elements in 3D, and the h-adaptive method is implemented to locally capture the boundary position.

Because structural topology optimization of compliant mechanisms results in non-convex optimization problems, it is hard to obtain the global optimum. To avoid the optimized structure falling into a bad local optimum too early due to the use of mesh adaptation, we use the following strategy for mesh discretization. Firstly, we use a relatively coarse mesh to start the optimization procedure, then we refine the mesh regularly within the whole design domain when the change of the objective value is smaller than certain small values. For example, if the change is smaller than 5 percent when compared with the value from the last iteration. This procedure is repeated twice until we obtain a relatively clear topology of the

structure. Then we use the h-adaptive method to locally refine the mesh in which the nodal density value is larger than a certain value, and coarsen the mesh where the nodal density value is smaller than a certain value (Fig. 21). In this procedure we assume that the final layout of the compliant mechanism is similar to the layout before we refine the mesh adaptively, because a high nodal design value cannot happen in a coarse mesh area as confirmed by our numerical experiments.

When compared with a rectangular mesh, the connectivity of an unstructured triangular (2D) or tetrahedral (3D) mesh is more complicated. Therefore, the filtering which is used to avoid numerical problems needs to be considered separately here. We use the idea of isotropic diffusion to obtain a filter matrix:

$$\frac{\partial \rho}{\partial t} = \nabla \cdot (\nabla \rho) \tag{24}$$

The discretized form of Eq. (24) is

$$\rho^{new} = \rho^{old} + \delta t M^{-1} K \tag{25}$$

where M is the mass matrix, K is the stiffness matrix, and δt is the discretized time step. Because the mesh is fixed for each hierarchic mesh, one can calculate the filter matrix $M^{-1}K$ once and use it to filter the sensitivity and density when the mesh remains unchanged. This method is used for optimization with a regularly refined mesh. After the design domain is adaptively refined, using an isotropic type filter does not result in a clear material-void structure. Therefore, we use the anisotropic diffusion method:

$$\frac{\partial \rho}{\partial t} = \beta \nabla \cdot \left(\frac{1}{1 + |\nabla \rho|^2} \nabla \rho \right) \tag{26}$$

where β is a small scalar number with positive value and t is the diffusion time (Fig. 17). The computational cost of solving the nonlinear equation (26) is very high. Instead of solving it in each optimization iteration, we solve it every 5–10 iterations without filtering either the sensitivity or the nodal density values between two anisotropic filtering steps. In this paper, all of the sensitivity analyses, mesh adaptation and the isotropic and anisotropic filtering steps are implemented using the commercial software Comsol's script version 3.3 [22]. The task of programming is detailed in [33].

5. Numerical examples

In this section, we illustrate our method using compliant gripper examples with multiple EDCs to control the output performance. The material used to design the compliant mechanisms in this paper has Young's modulus $E = 1.1$ GPa and Poisson's ratio $\nu = 0.35$.

5.1. Gripper design using single push force

The first example demonstrates the design procedure of the compliant grippers. The case of the design domain is $4 \times 3\,\text{cm}^2$ and the thickness is 1 mm (Fig. 1). The input load $f_{in} = 1$ N is applied at the center of the right edge. The volume is restricted to 20 percent of the design domain. Due to the symmetrical property, only the upper half of the design domain is discretized using triangular mesh. The optimized topology obtained without using equality constraint is shown in Fig. 6a. The resulting deformation obtained using linear FE analysis shows non-parallel movement of the gripper jaws (Fig. 6b). Using the optimization model (P1a) with one equality constraint for output displacement, and the sensitivity analysis method we proposed in this paper, the optimized topology is shown in

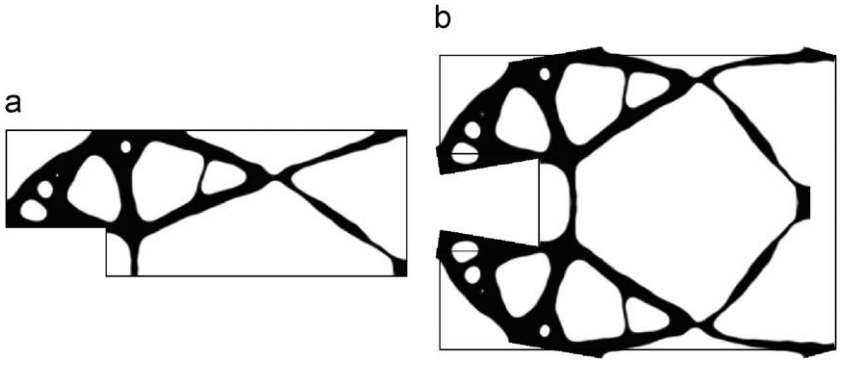

Fig. 6. Optimized compliant gripper using u_{out}/SE model in Fig. 5a without equality displacement constraint. (a) Optimized topology, (b) linear deformation analysis (scaled deformation).

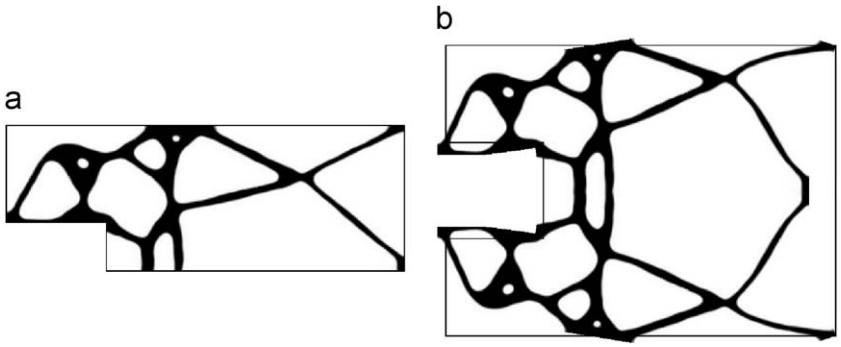

Fig. 7. Optimized compliant gripper using reaction force model in Fig. 5 with equality displacement constraint $u_{out} - u_{O2y} = 0$ (P1). (a) Optimized topology, (b) linear deformation analysis (scaled deformation). The ratio of y-displacement on two output points is $u_{out}/u_{O2y} = 1.029$.

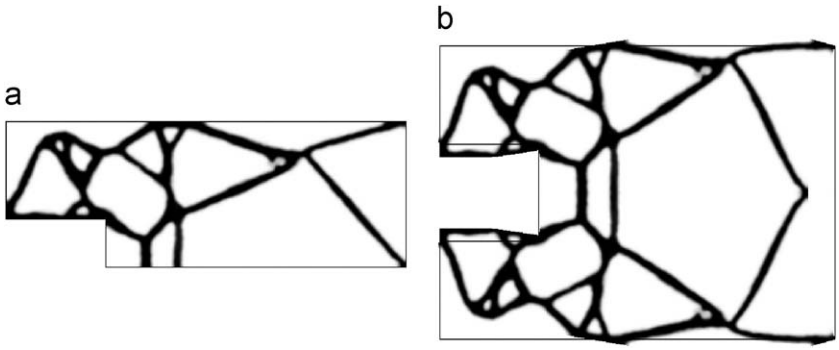

Fig. 8. Optimized compliant gripper using reaction force model in Fig. 5 with three equality displacement constraints, $u_{out} - u_{O2y} = 0$, $u_{O1x} = 0$, $u_{O2x} = 0$ (P2). (a) Optimized topology, (b) linear deformation analysis (scaled deformation). The ratio of y-displacement on two output points $u_{out}/u_{O2y} = 1.032$; the ratio $u_{O1x}/u_{O1y} = 0.017$, $u_{O2x}/u_{O2y} = 0.019$.

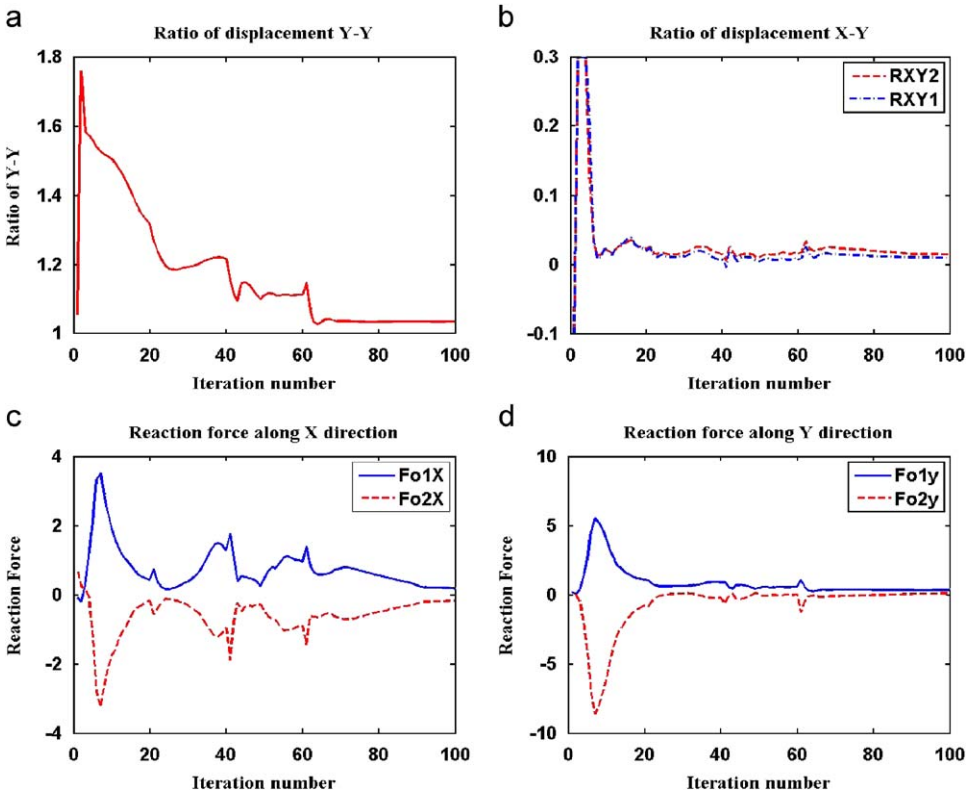

Fig. 9. Convergence curves for the compliant gripper in (Fig. 8). (a) The ratio of u_{out}/u_{O2y}, (b) the ratio of u_{O1x}/u_{O1y} (RXY1) and u_{O2x}/u_{O2y} (RXY2). For the value larger than 0.3 and smaller than −0.1 are cutoff in order to show the convergence curve clearly, (c) convergence curve of the artificial reaction forces $F_{o1x} = F_{RO1x}$ and $F_{o2x} = F_{RO2x}$ to implement constraints $u_{O1x} = u_{O2x} = 0$ on two output points, (d) convergence curve of the artificial reaction forces $F_{o1y} = F_{RO1y}$ and $F_{o2y} = F_{RO2y}$ to implement constraints $u_{O1y} = u_{O2y}$ on two output points.

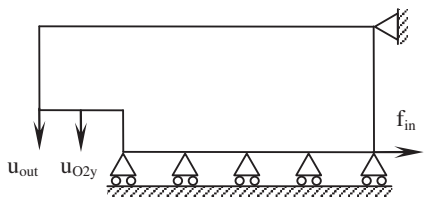

Fig. 10. Design domain with pull force on the right down corner.

Fig. 7a. The resulting deformation obtained using linear FE analysis (Fig. 7b) shows a nearly parallel movement of the gripper jaws. The ratio of output displacement at two points with equality constraints is 1.029, which means a 2.9 percent of deviation from the ideal ratio 1.0. To obtain a more precise control of output performance, the optimization model (P2) is used to design this compliant gripper. In this case, three different displacement equality constraints are used. The optimized topology is shown in Fig. 8a. The resulting deformation obtained using linear FE analysis (Fig. 8b) shows a vertical parallel movement of the gripper jaw. The ratio of output displacement at two output points is 1.032, which means 3.2 percent of constraints residual. The ratio of u_{Oix}/u_{Oiy} at two output points is 0.017 and 0.019, which is quite close to the ideal value zero. In Fig. 7b, the ratio of u_{Oix}/u_{Oiy} on two output points is 0.657 and 0.669, it means obvious horizontal displacement at two output points. From Figs. 7 and 8, it is clear that added constraints result in mechanisms with an en-

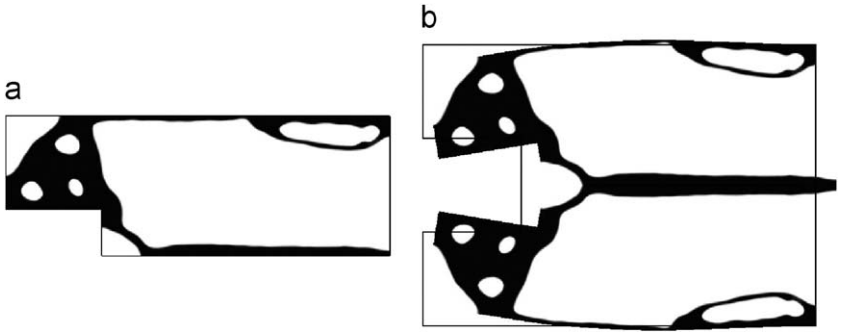

Fig. 11. Optimized compliant gripper using u_{out}/SE model in Fig. 10 without equality displacement constraint. (a) Optimized topology, (b) linear deformation analysis (scaled deformation).

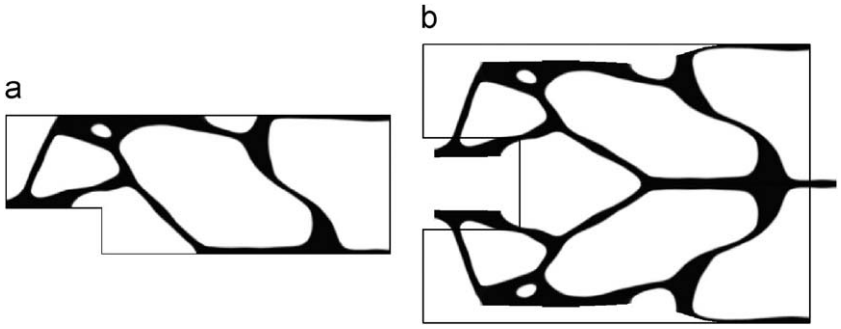

Fig. 12. Optimized compliant gripper using reaction force model in Fig. 10 with equality displacement constraint $u_{out} - u_{O2y} = 0$ (P1). (a) Optimized topology, (b) linear deformation analysis (scaled deformation). The ratio of y-displacement on two output points $u_{out}/u_{O2y} = 1.035$.

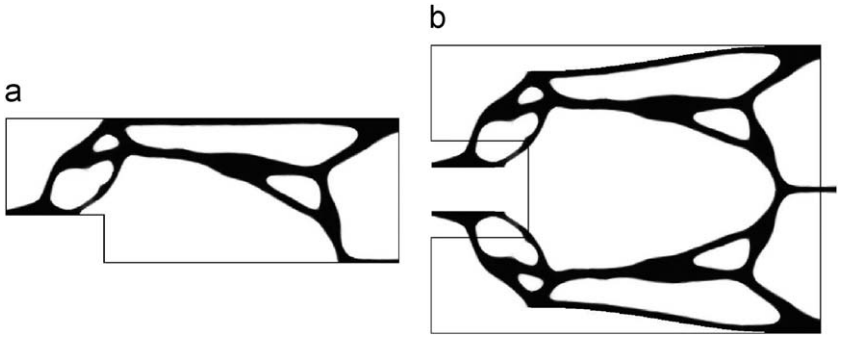

Fig. 13. Optimized compliant gripper using reaction force model in Fig. 10 with three equality displacement constraints, $u_{out} - u_{O2y} = 0$, $u_{O1x} = 0$, $u_{O2x} = 0$ (P2), using reaction force model. (a) Optimized topology, (b) linear deformation analysis (scaled deformation). The ratio of y-displacement on two output points $u_{out}/u_{O2y} = 1.015$; the ratio $u_{O1x}/u_{O1y} = 0.023$, $u_{O2x}/u_{O2y} = 0.023$.

tirely different topology. It is worth noting that the extra constraints in optimization model (P3) does not modify the ratio of output displacement and input displacement too much compared to the optimization model (P2), where the value of ratio u_{out}/u_{I1x} is 0.486 and 0.461, respectively. The performanceof the optimization procedure of the compliant gripper in Fig. 8a is shown in Fig. 9. Fig. 9c and d show that the reaction forces added at the points with equality constraints converge to zero as the constraints are satisfied gradually.

In these three examples, the design domain is discretized using 6578 triangular elements at the beginning of the optimization. The mesh is refined twice inside the design domain if the change of the value of the objective function is smaller than 5 percent when compared with the value from the last iteration. In order to obtain a smooth expression of the material boundary which can be used directly for CAD tools or fabrication, the h-adaptive refinement is used to refine the mesh locally around the material boundary. Consequently the number of finite elements used may vary for different examples in this paper. For the structural topology in Fig. 8a, two adaptive meshes which have 36 061 and 56 202 triangular elements are used. Therefore, the material boundary is quite smooth even for the monolithic slender structures (Fig. 21).

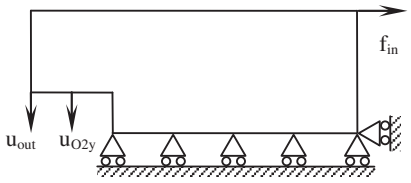

Fig. 14. Design domain with pull force on the up-right corner.

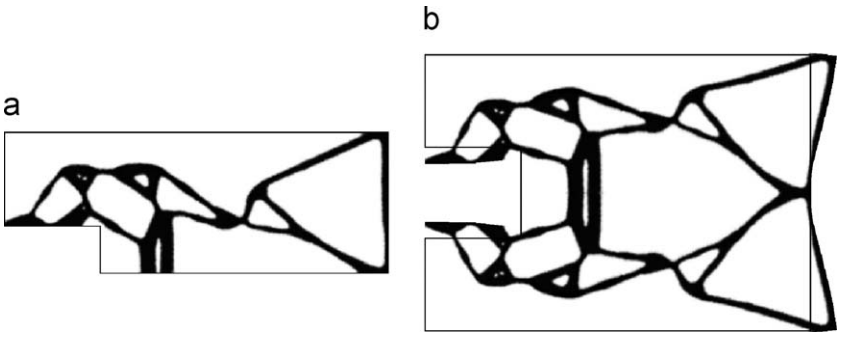

Fig. 15. Optimized compliant gripper using reaction force model in Fig. 14 with four equality displacement constraints, $u_{out} - u_{O2y} = 0$, $u_{O1x} = 0$, $u_{O2x} = 0$, and $u_{I1y} = 0$ using reaction force model. (a) Optimized topology, (b) linear deformation analysis (scaled deformation). The ratio of y-displacement on two output points $u_{out}/u_{O2y} = 1.033$; the ratio $u_{O1x}/u_{O1y} = -0.019$, $u_{O2x}/u_{O2y} = -0.024$, $u_{I1y}/u_{I1x} = -0.024$.

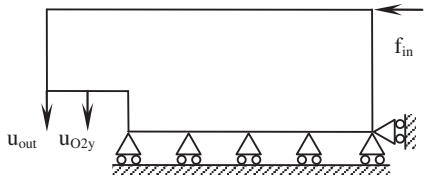

Fig. 16. Design domain with push force on the up-right corner.

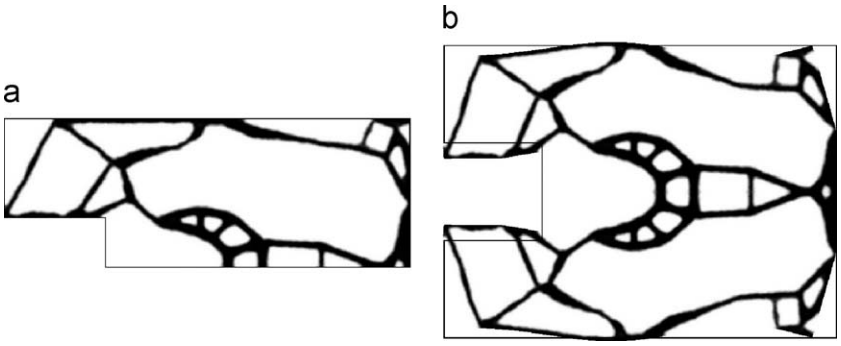

Fig. 17. Optimized compliant gripper using reaction force model in Fig. 16 with four equality displacement constraints, $u_{out} - u_{O2y} = 0$, $u_{O1x} = 0$, $u_{O2x} = 0$, and $u_{I1y} = 0$ using reaction force model. (a) Optimized topology, (b) linear deformation analysis (scaled deformation). The ratio of y-displacement on two output points $u_{O1y}/u_{O2y} = 1.038$; the ratio $u_{O1x}/u_{O1y} = 0.001$, $u_{O2x}/u_{O2y} = 0.004$, $u_{I1y}/u_{I1x} = -0.002$.

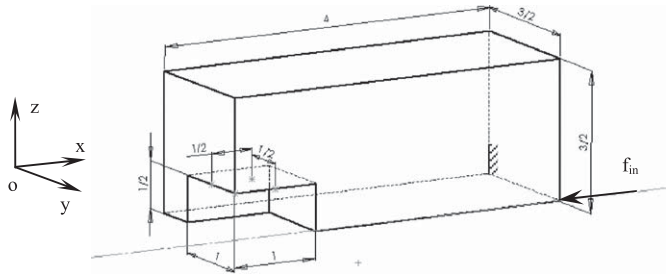

Fig. 18. One-quarter of design domain for 3D compliant gripper. Four star points are the output displacement points.

5.2. Gripper design using single pull force

Using the same design domain, material property, and optimization method, we design compliant grippers which have similar performance at the two output points but a push force $f_{in} = 1$ N is applied at the center of the right edge. The volume is restricted to 20 percent of the design domain. Due to symmetrical property, only the upper half of the design domain is discretized using triangular mesh. For the following three cases: (1) where there is no displacement constraint, (2) where there is one equality displacement constraint, and (3) where there are three equality displacement constraints, the optimization results are shown in Figs. 11, 12, and 13, respectively. In Fig. 12 the ratio of output displacements at two output points is 1.035, which means 3.5 percent of constraints residual. In Fig. 13 the ratio of output displacement at two output points is 1.015, which means 1.5 percent of constraints residual. The ratio of u_{Oix}/U_{Oiy} at two output points is 0.023 and 0.023, which are quite close to the ideal value zero.

5.3. Gripper design using symmetrical forces

When the input forces do not act along the symmetrical line of the design domain, the displacement on the input force point may also need additional constraints. For the same design domain, the input forces now act on the top and bottom corners of the right edge. The volume is restricted to 20 percent of the design domain. Due

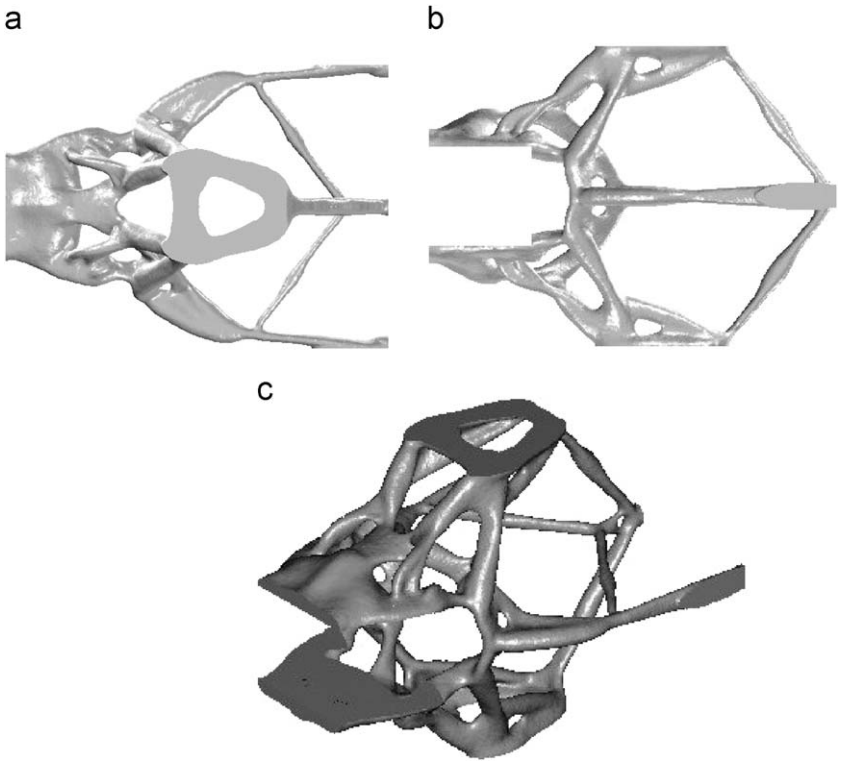

Fig. 19. Optimized result of the 3D compliant gripper. (a) *X*–*Y* profile view, (b) *X*–*Z* profile view, (c) 3D structure. The ratio of *z*-displacement on four output points are 1.019, 1.017, 1.005; the ratio u_{Oix}/u_{Oiz} are 0.075, 0.080, 0.081, 0.086, the ratio u_{Oiy}/u_{Oiz} are 0.003, −0.004.

to symmetrical property, only the upper half of the design domain is discretized using triangular mesh. In optimization model (P3) another equality constraint is added to limit the displacement along the direction which is perpendicular to the input load, for the design domain and pull input force shown in Fig. 14. The optimized topology is shown in Fig. 15. When the input force is push force (Fig. 16), the optimized topology is shown in Fig. 17. Based on the resulting deformation using linear FE analysis, the equality constraints are satisfied within small residual. The ratio of displacement at two output points in Fig. 15b is 1.033, which means 3.3 percent of constraints residual. The ratio of $u_{Oix}/_{Oiy}$ at two output points is −0.019 and −0.024, the ratio of u_{Iiy}/u_{Iix} at input force point is −0.024 which is both quite close to the ideal value zero. The ratio of output displacement at two output points in Fig. 17b is 1.038, which means 3.8 percent of constraints residual. The ratio of u_{Oix}/u_{Oiy} at two output points is 0.001 and 0.004, the ratio of U_{Iiy}/U_{Iix} at input force point is −0.002 which means both are quite close to the ideal value zero.

5.4. 3D gripper design

Compared with the 2D case, a 3D gripper (Figs. 18–20) may have more complicated topology. The size of design domain is $4\times3\times3\,\mathrm{cm}^3$ (Fig. 18), and input load $f_{in}=1N$ is applied at the center point of the right-side surface. Due to symmetrical property, only one quarter of the design domain is discretized using the tetrahedral element. The optimization model is P4. Here we impose constraints so that the gripper jaw can only close vertical and parallel. There are nine equality constraints, the first three limit the deformation along Z direction, another four limit the deformation along X direction, and the last two limit the deformation along the Y direction. The optimized topology is shown in Fig. 19. Fig. 19a and b are the X–Y and X–Z profile, respectively. The ratio of output displacement between four output points is 1.019, 1.017 and 1.005, respectively. The ratio

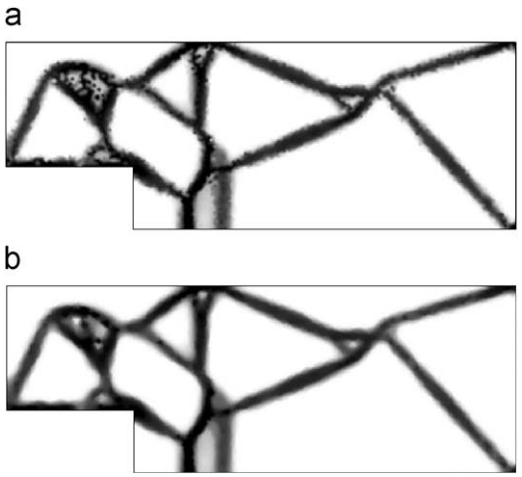

Fig. 20. Smoothing the numerical oscillation using anisotropic filter. (a) Numerical result with numerical oscillation, (b) smoothed result.

of u_{Oix}/u_{Oiz} at four output points is 0.075, 0.080, 0.081 and 0.086, respectively, and the ratio of u_{Oiy}/u_{Oiz} at two output points which are not located on the symmetrical profile, is 0.003 and −0.004, respectively, in which both are quite close to the ideal value zero (Fig. 19).

6. Discussion

From the point of view of application, it is preferable that the compliant mechanism can generate relatively large deformation under a load vector. Nonlinear deformation analysis is necessary in this case. In [10], the compliant mechanisms are designed using geometrically large deformation analysis. Numerical examples demonstrate

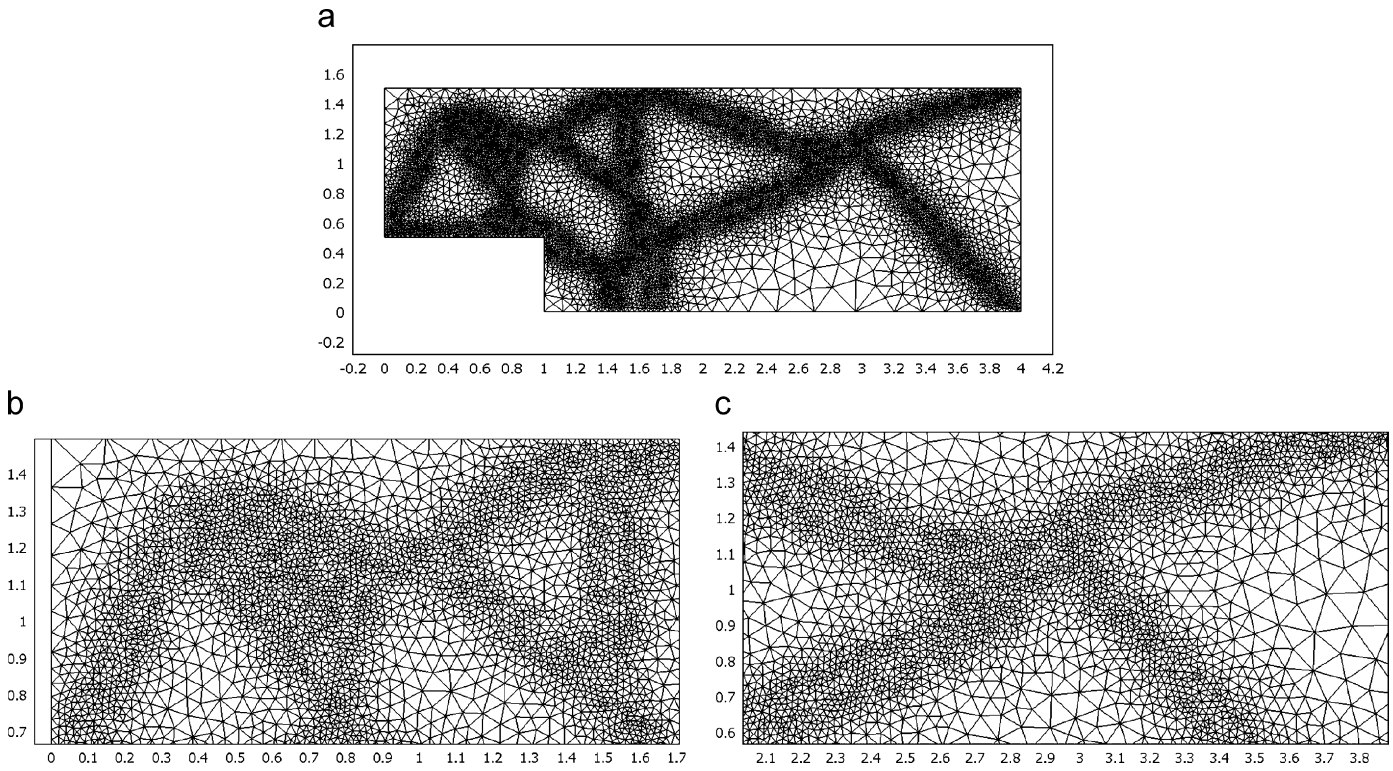

Fig. 21. (a) Adaptive mesh used for Fig. 8a. (b) and (c) Local enlarged mesh details.

that the optimal solution using linear small deformation analysis may fall into a suboptimal solution, in which the structural topology is different to the one which is optimized using geometrically large deformation analysis. In this paper, we focus on the algorithm which can implement displacement equality constraints, and only the linear small deformation analysis is used. To verify the optimal topology we obtained, one can compare the numerical results in [6] in which linear small deformation analysis is used. However, the method we proposed to deal with equality constraints can be extended to the geometrically large deformation analysis. The reasons are: (1) that the reaction force can be calculated in the same way as the linear case; (2) the adjoint vector can be calculated using the tangential stiffness matrix [10]. Of course, the performance of the algorithm we proposed in combination with nonlinear analysis deserves a detailed discussion in a separate paper.

In this paper, a mechanical problem subject to displacement equality constraints is considered. The method we proposed to deal with equality constraints can also be extended to other elliptical type partial differential equations, such as the electrostatic problem with equality potential constraints, and the thermal problem with equality temperature constraints, in which cases the corresponding physical meaning of the Lagrange multipliers are electrical charge and thermal flux.

Only equality constraints are considered in this paper. For more general structural optimization problems, inequality displacement constraint should also be considered. One possible way of extending our method to inequality displacement constraints is to choose the active inequality constraints set and then transfer these to the equality constraints set after solving the original forward problem.

7. Conclusion

In order to obtain a desired input and output displacement performance, compliant mechanisms design requires the consideration of multiple displacement constraints. Based on artificial reaction forces, we propose a method which can be used to design compliant mechanism with multiple equality displacement constraints. Numerical examples illustrate the effect of the method. If there is only a few equality displacement constraints, the computational cost of the sensitivity is expensive when comparing with the MMA type method. However, the advantage of the method we propose is that one can implement more equality constraints at many points without increasing the computational cost excessively.

Acknowledgment

This work is supported by CIOMP innovation fund and German Research Foundation (DFG) 1883/9-1.

References

[1] G.K. Ananthasuresh, Optimal Synthesis Methods for MEMS, Kluwer Academic Publishers, Boston, 2003.
[2] S. Kota, J. Hetrick, Z. Li, L. Saggere, Tailoring unconventional actuators using compliant transmissions: Design methods and applications, IEEE/ASME Transactions on Mechatronics 4 (1999) 396–408.
[3] M.P. Bendsoe, O. Sigmund, Topology Optimization Theory, Methods and Applications, Springer, Berlin, 2003.
[4] G.K. Ananthasuresh, S. Kota, Designing compliant mechanisms, Mechanical Engineering 117 (1995) 93–96.
[5] M. Frecker, G.K. Ananthasuresh, S. Nishiwaki, N. Kikuchi, S. Kota, Topological synthesis of compliant mechanisms using multi-criteria optimization, ASME Journal of Mechanical Design 119 (1997) 238–245.
[6] O. Sigmund, On the design of compliant mechanisms using topology optimization, Mechanics of Structures and Machines 25 (1997) 495–526.
[7] O. Sigmund, Design of multiphysics actuators using topology optimization—Part I: one-material structures, Computer Method in Applied Mechanics and Engineering 190 (2001) 6577–6604.
[8] A. Saxena, G.K. Ananthasuresh, On an optimal property of compliant topologies, Structural and Multidisciplinary Optimization 19 (2001) 36–49.
[9] I.Y. Kim, O.L. de Weck, Adaptive weighted-sum method for bi-objective optimization: Pareto front generation, Structural and Multidisciplinary Optimization 29 (2005) 149–158.

[10] C.B.W. Pedersen, T. Buhl, O. Sigmund, Topology synthesis of large-displacement compliant mechanisms, International Journal for Numerical Methods in Engineering 50 (2001) 2683–2705.
[11] K. Svanberg, The method of moving asymptotes: a new method for structural optimization, International Journal for Numerical Method in Engineering 24 (1987) 359–373.
[12] C. Fleury, CONLIN: an efficient dual optimizer based on convex approximation concepts, Structural Optimization 1 (1989) 81–89.
[13] W.H. Zhang, C. Fleury, P. Duysinx, A generalized method of moving asymptotes (GMMA) including equality constraints, Structural Optimization 12 (1996) 143–146.
[14] M. Bruyneel, P. Duysinx, C. Fleury, A family of MMA approximations for structural optimization, Structural Multidisciplinary Optimization 24 (2002) 263–276.
[15] R. Parsons, S.L. Canfield, Developing genetic programming techniques for the design of compliant mechanisms, Structural Multidisciplinary Optimization 24 (2002) 78–86.
[16] A. Saxena, Topology design of large displacement compliant mechanisms with multiple materials and multiple output ports, Structural Multidisciplinary Optimization 30 (2005) 477–490.
[17] S.F. Rahmatalla, C.C. Swan, Sparse monolithic compliant mechanisms using continuum structural topology optimization, International Journal for Numerical Method in Engineering 62 (2005) 1579–1605.
[18] J. Nocedal, S.J. Wright, Numerical Optimization, Springer, Berlin, 1999.
[19] O. Sigmund, J. Petersson, Numerical instabilities in topology optimization: a survey on procedures dealing with checkerboards, mesh-dependencies and local minimal, Structural Optimization 16 (1998) 68–75.
[20] T. Borrvall, J. Petersson, Topology optimization using regularized intermediate density control, Computer Method in Applied Mechanics and Engineering 190 (2001) 4911–4928.
[21] O.C. Zienkiewicz, R. Taylor, J. Zhu, The Finite Element Method, Elsevier, Amsterdam, 2005.
[22] ⟨http://www.comsol.com⟩.
[23] S.F. Rahmatalla, C.C. Swan, A Q4/Q4 continuum structural topology optimization implementation, Structural Multidisciplinary Optimization 27 (2004) 130–135.
[24] O. Sigmund, A 99 line topology optimization code written in Matlab, Structural Multidisciplinary Optimization 21 (2001) 120–127.
[25] M.P. Bendsoe, Optimization of Structural Topology, Shape and Material, Springer, Berlin, 1995.
[28] C. Johnson, Numerical Solution of Partial Differential Equations by the Finite Element Method, Cambridge University Press, Cambridge, 1988.
[29] A. Pantano, R.C. Averill, A penalty-based finite element interface technology, Computers & Structures 80 (2002) 1725–1748.
[32] J. Costa, M.K. Alves, Layout optimization with H-adaptivity of structures, International Journal for Numerical Methods in Engineering 58 (2003) 83–102.
[33] B. Lemke, Z. Liu, J.G. Korvink, Structural topology optimization using COMSOL, in: COMSOL conference, 2006.